Lagrangian Frequency Spectrum as a Diagnostic for Magnetohydrodynamic Turbulence Dynamics

Angela Busse* and Wolf-Christian Müller†
Max-Planck-Institut für Plasmaphysik, Boltzmannstraße 2, 85748 Garching bei München, Germany

Grigol Gogoberidze‡
Georgian National Astrophysical Observatory, 2a Kazbegi Avenue, 0160 Tbilisi, Georgia
and Centre for Plasma Astrophysics, University of Leuven, B-3001 Leuven, Belgium
(Received 6 September 2010; published 3 December 2010)

For the phenomenological description of magnetohydrodynamic turbulence competing models exist, e.g., Boldyrev [Phys. Rev. Lett. **96**, 115002 (2006)] and Gogoberidze [Phys. Plasmas **14**, 022304 (2007)], which predict the same Eulerian inertial-range scaling of the turbulent energy spectrum although they employ fundamentally different basic interaction mechanisms. A relation is found that links the Lagrangian frequency spectrum with the autocorrelation time scale of the turbulent fluctuations τ_{ac} and the associated cascade time scale τ_{cas}. Thus, the Lagrangian energy spectrum can serve to identify weak ($\tau_{ac} \ll \tau_{cas}$) and strong ($\tau_{ac} \sim \tau_{cas}$) interaction mechanisms providing insight into the turbulent energy cascade. The new approach is illustrated by results from direct numerical simulations of two- and three-dimensional incompressible MHD turbulence.

DOI: 10.1103/PhysRevLett.105.235005 PACS numbers: 52.30.Cv, 47.10.−g, 47.27.Gs, 52.35.Ra

Magnetohydrodynamic (MHD) turbulence has been the subject of intense research during the last decades since turbulent low-frequency, long-wavelength fluctuations conveniently described in the incompressible MHD framework are present in many astrophysical systems (see, for example, [1] and references therein). As of now, the theoretical description of the universal statistical properties of turbulent flows relies mainly on phenomenological models like Kolmogorov's K41 picture [2] of hydrodynamic turbulence. In the incompressible MHD case the phenomenological description is complicated by the presence of shear Alfvén wave modes and their associated time scale, the Alfvén-time τ_A. Especially for turbulence in the presence of a strong mean magnetic field there exist competing phenomenological models of the inertial-range energy cascade [3–7]. Although based on physically different mechanisms the most recent models by Boldyrev [6] and Gogoberidze [7] predict identical diagnostic signatures, e.g., the same inertial-range scaling of the energy spectrum, and are thus hardly distinguishable by conventional measurements in the Eulerian frame of reference. Complementing Eulerian diagnostics, the Lagrangian frequency spectrum gives insight into the time scales associated with the turbulent energy cascade and the underlying nonlinear interactions of turbulent fluctuations.

This Letter reports a fundamental relation between the Lagrangian frequency spectrum and the characteristic time scales of turbulence, the autocorrelation time τ_{ac}, and the cascade time τ_{cas}. Here, the autocorrelation time $\tau_{ac} = \tau_{ac}(\ell)$ characterizes the dominant nonlinear interaction process between turbulent fluctuations with ℓ being the spatial scale under consideration. On the cascade time scale τ_{cas} the fluctuations at a fixed spatial scale loose their coherence and decay into smaller turbulent fluctuations. The relation presented in the following allows us to investigate a fundamental aspect of turbulent dynamics, i.e., to distinguish whether nonlinear interactions are weak, $\tau_{ac} \ll \tau_{cas}$, or strong $\tau_{ac} \sim \tau_{cas}$. The relation is supported by high-Reynolds-number direct numerical simulations of two- and three-dimensional MHD turbulence. In the following, pertinent turbulence phenomenologies are summarized focusing on their characteristic time scales.

In the K41 picture of Navier-Stokes turbulence the autocorrelation time scale τ_{ac} is determined dimensionally by the nonlinear turnover time $\tau_{NL} = \ell/v_\ell$ where v_ℓ is a velocity fluctuation (eddy) at scale ℓ. A single nonlinear interaction between eddies reduces the coherence of an involved fluctuation so significantly that it ceases to exist at scale ℓ having generated fluctuations at slightly smaller scales. The required time for the associated decorrelation in the K41 picture is $\tau_{cas} \sim \tau_{NL} \sim \tau_{ac}$; thus the nonlinear interaction is strong. In incompressible two-dimensional MHD turbulence the Iroshnikov-Kraichnan (IK) phenomenology [3,4] seems to apply; see, e.g., [8]. There, colliding counterpropagating Alfvénic fluctuations lead to a wave-based nonlinear decorrelation of turbulent structures. The fundamental interaction time scale is the Alfvén-time $\tau_A = \ell/b_0$ where the assumption of constant mass density yields the Alfvén speed as the value of a properly normalized external magnetic guide field b_0 or, if no such field is present, the slowly varying large-scale magnetic fluctuations b_{rms}. As colliding Alfvén wave packets experience only a small deformation in a single nonlinear interaction, many consecutive interactions are required for a cascade

step, i.e., $\tau_A \ll \tau_{\mathrm{NL}}^2/\tau_A \sim \tau_{\mathrm{cas}}$ since generally $\tau_A \ll \tau_{\mathrm{NL}}$, and the nonlinear interaction is weak. In incompressible three-dimensional MHD turbulence with weak to moderate mean magnetic field the Goldreich-Sridhar (GS) [5] phenomenology has become widely accepted. It enhances the IK picture by explicitly taking into account dynamical anisotropy with regard to the direction of the local magnetic field. In addition, the hypothesis of a critical balance of turnover and Alfvén time is made, i.e., $\tau_{\mathrm{ac}} \sim \tau_A \sim \tau_{\mathrm{NL}} \sim \tau_{\mathrm{cas}}$ resulting in strong nonlinear interaction.

However, the inertial-range scaling of the Eulerian energy spectrum of MHD turbulence in a strong mean magnetic field does not agree with the GS phenomenology [9–13]. A proposed alternative is the dynamic-alignment model (DA) [6] which extends the GS model by a scale-dependent polarization of the interacting wave packets but still leads to strong nonlinear interaction. By a different approach, an anisotropic variant of the IK picture (AIK) [7] yields weak interaction dynamics. It proposes nonlocal decorrelation effects on inertial-range scales by large-scale fluctuations. Both phenomenologies lead to identical scaling results with regard to Eulerian two-point statistics although their underlying physical assumptions are fundamentally different.

The inertial-range scaling of the Eulerian energy spectrum $E(k)$ serves as a standard diagnostic for turbulence investigations, but is in fact not unique: the K41 and GS models yield $E(k) \sim k^{-5/3}$. In the GS picture the wave number k is defined in a direction perpendicular to the magnetic field $k \rightarrow k_\perp$. The DA, AIK, and IK models, in contrast, all predict $E(k) \sim k^{-3/2}$ with $k \rightarrow k_\perp$ for DA and AIK. This has motivated the development of a new diagnostic approach that allows us to probe the relation between τ_{ac} and τ_{cas} as presented in the following.

The Lagrangian two-point two-time velocity correlation [14] is defined as

$$R_L = \langle \boldsymbol{V}(\boldsymbol{X}_0 + \boldsymbol{r}, \tau + t_0) \cdot \boldsymbol{V}(\boldsymbol{X}_0, t_0) \rangle, \tag{1}$$

where $\boldsymbol{V}(\boldsymbol{X}_0 + \boldsymbol{r}, t_0 + \tau)$ is the velocity measured at time $t_0 + \tau$ of a fluid element that was at position $\boldsymbol{X}_0 + \boldsymbol{r}$ at time t_0. The Lagrangian variable $\boldsymbol{X} = \boldsymbol{X}(\boldsymbol{X}_0, t)$ is the time-dependent position along a fluid particle's trajectory. The Lagrangian velocity $\boldsymbol{V}(\boldsymbol{X}_0, t)$ is connected to the Eulerian velocity field by $\boldsymbol{V}(\boldsymbol{X}_0, t) = \boldsymbol{v}(\boldsymbol{x} = \boldsymbol{X}(\boldsymbol{X}_0, t), t)$. While R_L is generally a correlation function involving two fluid particles at positions $\boldsymbol{X}^{(1)}(\boldsymbol{X}_0 + \boldsymbol{r}, \tau + t_0)$ and $\boldsymbol{X}^{(2)}(\boldsymbol{X}_0, t_0)$ it reduces to a two-point velocity correlation along a single trajectory if $\boldsymbol{r} = 0$. The corresponding Eulerian correlation function is

$$R_E = \langle \boldsymbol{v}(\boldsymbol{x} + \boldsymbol{r}, t + \tau) \cdot \boldsymbol{v}(\boldsymbol{x}, t) \rangle, \tag{2}$$

with $\boldsymbol{v}(\boldsymbol{x}, t)$ representing the velocity field at a position $\boldsymbol{x}$ and time t while $\boldsymbol{r}$ and τ stand for independent translations in space and time, respectively.

For statistically homogeneous and stationary turbulence these functions depend on $\boldsymbol{r}$ and τ only, $R_{L,E} = R_{L,E}(\boldsymbol{r}, \tau)$. The corresponding two-time spectral functions $Q(\boldsymbol{k}, \tau)$ are defined as the Fourier transforms of the correlation functions

$$R_{L,E} = \int d^3\boldsymbol{k} \exp(i\boldsymbol{k} \cdot \boldsymbol{r}) Q_{L,E}(\boldsymbol{k}, \tau). \tag{3}$$

The two-time spectral functions are related to the three-dimensional energy spectrum $E(\boldsymbol{k})$ by

$$Q_{L,E}(\boldsymbol{k}, \tau) = E(\boldsymbol{k}) G_{L,E}(\tau/\tau_{\mathrm{ac}}^{L,E}), \tag{4}$$

where $\tau_{\mathrm{ac}}^{L,E}$ are the Lagrangian and Eulerian autocorrelation time scales, and $G_{L,E}(\tau/\tau_{\mathrm{ac}}^{L,E})$ are the corresponding response functions [15]. The general features of models of the response function used in the theoretical description of turbulence [15–17] are that $G_{L,E}$ is a smooth function with $G_{L,E}(0) = 1$, $G_{L,E}(x) = 0$ for $x \gg 0$ and $\int_0^\infty G_{L,E}(x)dx = 1$.

The Lagrangian and Eulerian frequency spectra are defined as [14]

$$\Phi_{L,E}(\omega) = \frac{1}{2\pi} \int d\tau \cos(\omega\tau) R_{L,E}(0, \tau). \tag{5}$$

Putting Eq. (4) into Eq. (3), and plugging the result in Eq. (5) yields for the frequency spectrum

$$\Phi_{L,E}(\omega) = \frac{1}{\pi} \int d\tau \int dk E(k) G_{L,E}(\tau/\tau_{\mathrm{ac}}^{L,E}) \cos(\omega\tau), \tag{6}$$

with $E^{\mathrm{total}} = \int dk E(k)$. The energy spectrum $E(k)$ and the associated wave number has to be defined in a suitable way for the considered geometry, e.g., spherical, planar, or cylindrical. Under the assumption of self-similarity of all involved dependent variables a dimensional approximation of this result linking wave number and frequency energy spectra in a simple way yields

$$\omega \Phi_{L,E}(\omega) \sim kE(k) \quad \text{with} \quad \omega \sim 1/\tau_{\mathrm{ac}}^{L,E}(k). \tag{7}$$

Note that relation (7) is also found in [18] following a different and more specific approach.

The Eulerian correlation time at a fixed position is dominated by the sweeping of small-scale fluctuations by the largest-scale eddies $\tau_{\mathrm{ac}}^E \sim (kv_0)^{-1}$. Consequently, the spectral scaling of frequency and wave number spectra should be identical in this case with $\Phi_E^{\mathrm{GS}}(\omega) \sim (\varepsilon v_0)^{2/3}\omega^{-5/3}$ or $\Phi_E^{\mathrm{IK}}(\omega) \sim \varepsilon^{1/2} v_0 \omega^{-3/2}$ where the choice depends on the respective Eulerian inertial-range scaling. For MHD turbulence, however, the Lagrangian frequency spectrum allows us to distinguish turbulence phenomenologies based on strong nonlinear interaction such as GS and DA from pictures based on inherently weak interaction like (A)IK. Here, the Lagrangian autocorrelation time is assumed to be characteristic for nonlinear interactions in the energy cascade. In the MHD case, this holds as long as spectral kinetic and magnetic energy are sufficiently close to equipartition. A detailed investigation of the influence of the large wave number contribution of the Eulerian spectrum on the Lagrangian inertial range [14] shows that the

TABLE I. Parameters of the numerical simulations. Re: Reynolds number, $u_{\rm rms}$; $b_{\rm rms}$: rms value of velocity and magnetic field fluctuations; b_0: external mean magnetic field; ε^K, ε^M: kinetic and magnetic energy dissipation rates; ν kinematic viscosity; $N_{\rm colloc}$: numerical resolution.

Re	$u_{\rm rms}$	$b_{\rm rms}$	b_0	ε^K	ε^M	ν	$N_{\rm colloc}$
2150	0.75	0.93	0	6.4×10^{-2}	9.7×10^{-2}	5×10^{-4}	1024^2
6200	0.80	0.98	0	7.2×10^{-2}	1.0×10^{-1}	1.8×10^{-4}	2048^2
18 240	0.80	0.98	0	6.8×10^{-2}	8.9×10^{-2}	6×10^{-5}	4096^2
1050	0.44	0.59	0	0.11	0.17	1×10^{-3}	512^3
3150	0.46	0.64	0	0.12	0.17	3.4×10^{-4}	1024^3
1790	0.53	0.62	5	7.4×10^{-2}	8.5×10^{-2}	8×10^{-4}	$512^2 \times 256$
4410	0.55	0.63	5	7.7×10^{-2}	8.8×10^{-2}	3.3×10^{-4}	$1024^2 \times 512$

scaling of the Lagrangian inertial range is not adulterated by the Eulerian large-scale interval.

With $\omega \sim 1/\tau^L_{\rm ac}(k)$ and $E(\ell) \sim \omega \Phi_L(\omega)$, the classical constant-flux ansatz $E(\ell)/\tau_{\rm cas} \sim \varepsilon$ gives $\Phi_L(\omega) \sim \varepsilon \tau_{\rm cas} \tau^L_{\rm ac}$. Strong interaction turbulence is characterized by $\tau_{\rm ac} \sim \tau_{\rm cas}$ resulting in

$$\Phi_L(\omega) \sim \varepsilon \omega^{-2}. \tag{8}$$

This scaling is thus expected for the GS and the DA model and is well known from Navier-Stokes turbulence [19,20]. In contrast, for IK-based phenomenologies with a weak interaction mechanism $\tau_{\rm ac} \ll \tau_{\rm cas} \sim \tau^2_{\rm NL}/\tau^L_{\rm ac}$. Using relation (7), $\tau^L_{\rm ac} \sim \omega^{-1} \sim (k b_0)^{-1}$, and $\tau_{\rm NL} \sim (k^3 E_k)^{-1/2}$ yields $\tau_{\rm cas} \sim b_0^2 \Phi_L^{-1} \omega^{-2}$. Thus

$$\Phi_L(\omega) \sim \varepsilon^{1/2} b_0 \omega^{-3/2}. \tag{9}$$

Note that this result holds for IK. In the case of AIK the quasiconstant large-scale magnetic field b_0 has to be replaced by $v_{\rm rms}$.

Lagrangian frequency spectra are obtained by tracking fluid particles in direct numerical pseudospectral simulations of MHD turbulence. Details of the numerical method can be found in [9,21]. In the three-dimensional simulations the number of tracers amounts to 3.2×10^6, except for the lowest resolution runs where it is lowered to 5×10^5. In the two-dimensional simulations 2×10^6 tracers have been tracked. Important parameters and characteristics of the simulations are listed in Table I. The magnetic Prandtl number Pr_m, the ratio of kinematic viscosity ν to magnetic diffusivity η, is unity. Significant deviations from this value would lead to a degradation of observable inertial-range self-similarity due to numerical resolution constraints and are thus not considered here. In the macroscopically isotropic cases, $b_0 = 0$, both the magnetic and velocity field are forced by independent Ornstein-Uhlenbeck processes [22,23] in the wave number shell $k_f = 3$ in order to maintain quasistationary turbulence. In the anisotropic MHD case, $b_0 = 5$, large-scale Alfvénic fluctuations are excited by the stochastic forcing method which impair the frequency scaling range. Therefore in this case the system is forced by freezing the lowest wave number modes of the velocity and magnetic field of a fully developed turbulent state, see, e.g., [11]. In the two-dimensional case turbulence is maintained by keeping the kinetic and magnetic energy in the lowest wave number shells $1 \le |k| < 3 = k_f$ at a constant value. Based on the estimate $(L_0/\ell_{\rm diss})^{4/3}$ for the width of the inertial range, the Reynolds number is defined as $\mathrm{Re} = [2\pi/(k_f \ell_{\rm diss})]^{4/3}$ where $\ell_{\rm diss} \sim (\nu^3/\varepsilon^K)^{1/4}$ is the Kolmogorov dissipation length. To obtain the Lagrangian frequency spectrum first the autocorrelations of the velocity and the magnetic field fluctuations along the particle trajectories are calculated. The spectrum is then computed as the cosine transform of the autocorrelation functions [24]

$$\Phi_{L,i}(\omega) = \frac{1}{2\pi} \int d\tau \big(\langle V_i(t+\tau) V_i(t) \rangle + \langle b_i(t+\tau) b_i(t) \rangle \big) \cos(\omega \tau). \tag{10}$$

In the macroscopically isotropic MHD cases the frequency spectrum does not depend on the component i of the velocity or the magnetic field fluctuations. Here the total frequency spectrum $\Phi(\omega) = \sum_{i=1}^3 \Phi_i(\omega)$ is shown. In the

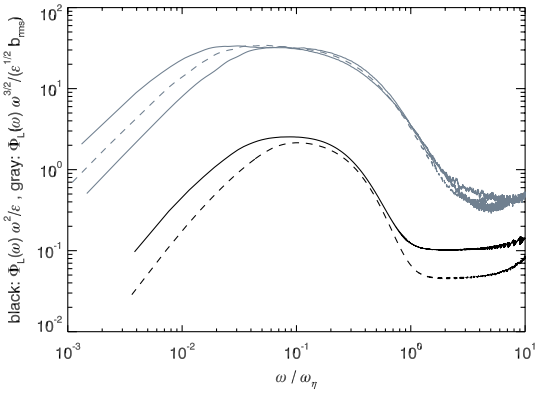

FIG. 1 (color online). The compensated Lagrangian frequency spectra in the macroscopically isotropic three-dimensional (black lines, compensated by ω^2/ε) and two-dimensional [gray lines, compensated by $\omega^{3/2}/(\varepsilon^{1/2} b_{\rm rms})$] cases for various Reynolds numbers: 1050 (black dashed), 3150 (black continuous), 2150 (gray dash-dotted), 6200 (gray dashed) and 18 240 (gray continuous). The frequency axis is normalized by the Kolmogorov frequency $\omega_\eta = \pi \sqrt{\epsilon^K/\nu}$. For clarity the spectra for the two-dimensional cases have been shifted by a constant factor.

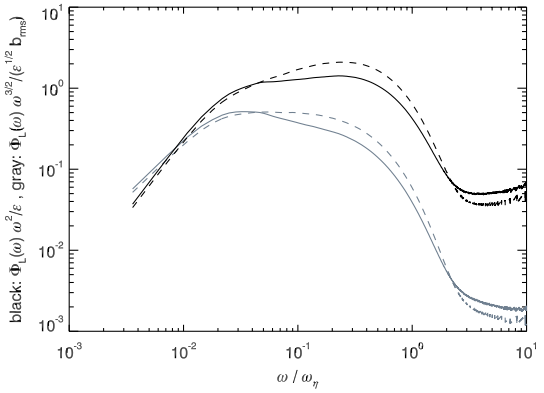

FIG. 2 (color online). The compensated Lagrangian frequency spectrum (cf. caption of Fig. 1) in the MHD case with a strong mean magnetic field for Reynolds numbers of about 4410 (cf. Table I). Continuous lines: $\boldsymbol{b}_0$-perpendicular components; dashed lines $\boldsymbol{b}_0$-parallel component.

hydrodynamic case (not shown) the spectrum scales as ω^{-2} in the inertial range in agreement with previous experimental [25] and numerical [20] results. In the macroscopically isotropic 3D MHD case the Lagrangian frequency spectrum also shows a scaling with ω^{-2} (see Fig. 1). This supports the GS phenomenology with its strong cascade mechanism for this configuration. In contrast, the Lagrangian spectra from the two-dimensional simulations which are shown in the same figure display an approximate $\omega^{-3/2}$ scaling indicative of a weak interaction cascade. This observation corroborates the IK phenomenology for the two-dimensional configuration. In the anisotropic MHD case a dependence of the scaling on the component of the fluctuations is observed (see Fig. 2). For the component along $\boldsymbol{b}_0$ $\omega^{-3/2}$ scaling is observed, whereas for the perpendicular components a scaling exponent $\alpha = 1.8 \pm 0.1$ [where $\Phi(\omega) \sim \omega^{-\alpha}$] is measured. This suggests that either the energy cascade changes its dynamical character from weak interaction (field parallel) to strong interaction (field perpendicular), or that the energetic structure of the flow cannot be captured adequately by a simple decomposition in parallel and perpendicular components.

In summary, a new relation is introduced that relates the nonlinear autocorrelation time and the cascade time of turbulence with the Lagrangian frequency spectrum. The relation is corroborated by comparing high-Reynolds-number direct numerical simulations of two- and three-dimensional MHD turbulence with currently accepted phenomenological expectations. As the Lagrangian frequency spectrum is sensitive to the underlying cascade mechanism it provides additional insight in the yet not fully understood case of MHD turbulence in a strong mean magnetic field. This is particularly useful in cases where the discrimination between different theoretical models of turbulence is hard or even impossible to achieve by Eulerian two-point statistics. The ability to investigate basic characteristics of turbulent energy transfer adds significant value to this approach.

The work of G. G. was supported by Georgian NSF Grant No. ST06/4096 and INTAS Grant No. 06-1000017-9258.

*angela.busse@ipp.mpg.de
Present address: University of Southampton, Southampton, U.K.
†wolf.mueller@ipp.mpg.de
‡gogober@geo.net.ge

[1] D. Biskamp, *Magnetohydrodynamic Turbulence* (Cambridge University Press, Cambridge, 2003).
[2] U. Frisch, *Turbulence* (Cambridge University Press, Cambridge, 1996).
[3] P. S. Iroshnikov, Astron. Zh. **40**, 742 (1963).[Sov. Astron. **7**, 566 (1964)].
[4] R. H. Kraichnan, Phys. Fluids **8**, 1385 (1965).
[5] P. Goldreich and S. Sridhar, Astrophys. J. **438**, 763 (1995).
[6] S. Boldyrev, Phys. Rev. Lett. **96**, 115002 (2006).
[7] G. Gogoberidze, Phys. Plasmas **14**, 022304 (2007).
[8] D. Biskamp and H. Welter, Phys. Fluids B **1**, 1964 (1989).
[9] W.-C. Müller, D. Biskamp, and R. Grappin, Phys. Rev. E **67**, 066302 (2003).
[10] J. Maron and P. Goldreich, Astrophys. J. **554**, 1175 (2001).
[11] W.-C. Müller and R. Grappin, Phys. Rev. Lett. **95**, 114502 (2005).
[12] J. Mason, F. Cattaneo, and S. Boldyrev, Phys. Rev. E **77**, 036403 (2008).
[13] J. C. Perez and S. Boldyrev, Phys. Rev. Lett. **102**, 025003 (2009).
[14] Y. Kaneda, Phys. Fluids A **5**, 2835 (1993).
[15] D. C. Leslie, *Developments in the Theory of Turbulence* (Clarendon Press, Oxford, 1983).
[16] R. H. Kraichnan, J. Fluid Mech. **5**, 497 (1959).
[17] S. F. Edwards, J. Fluid Mech. **18**, 239 (1964).
[18] H. Tennekes and J. L. Lumley, *A First Course in Turbulence* (MIT Press, Cambridge, MA, 1972), p. 277.
[19] H. Tennekes, J. Fluid Mech. **67**, 561 (1975).
[20] P. K. Yeung, S. B. Pope, and B. L. Sawford, J. Turbul. **7**, 1 (2006).
[21] A. Busse, W.-C. Müller, H. Homann, and R. Grauer, Phys. Plasmas **14**, 122303 (2007).
[22] G. E. Uhlenbeck and L. S. Ornstein, Phys. Rev. **36**, 823 (1930).
[23] V. Eswaran and S. B. Pope, Comput. Fluids **16**, 257 (1988).
[24] P. K. Yeung and S. B. Pope, J. Comput. Phys. **79**, 373 (1988).
[25] N. Mordant, E. Lévêque, and J.-F. Pinton, New J. Phys. **6**, 116 (2004).